Watt-Level Ka-Band Quasi-Optical Amplifier Arrays

Michael Forman, Todd Marshall, and Zoya Popović

Department of Electrical and Computer Engineering
University of Colorado
Boulder, CO 80309-0425

Phone: 303-492-8998
Fax: 303-492-5323
Email: forman@Colorado.EDU

Abstract

Small-signal gain, resonant-mode gain, and saturated output power are studied on two Ka-band quasi-optical slot-antenna amplifier arrays fabricated with commercial MMICs on aluminum-nitride substrates. The amplifier arrays have small-signal gains of 2.2 dB at 30.40 GHz and 6.5 dB at 31.40 GHz, respectively. In resonant mode, the amplifiers have small-signal gains of 10.7 dB at 31.52 GHz and 11.8 dB at 31.47 GHz. In saturation, the arrays both deliver 140 W EIRP or 0.5 W of output power at 30.40 GHz and 31.15 GHz.

I. Introduction

The motivation for quasi-optical amplifier power combining is to obtain watt power levels from solid-state amplifiers at millimeter-wave frequencies while taking advantage of high combining efficiency [1] and graceful degradation [2]. Several researchers have demonstrated Ka-band quasi-optical amplifier arrays: in [3], MMIC amplifiers were combined using slot antennas with up to 2.4 W of output power and 6 dB of small-signal gain; in [4] and [5], monolithic grid amplifiers, using HBTs and PHEMTs respectively, showed gain up to 60 GHz; and in [6], 1 W of power was obtained in an array mounted in a waveguide.

In this work, small-signal gain, resonant-mode gain, and saturated output power are presented on two experimental Ka-band arrays (referred to as Array A and Array B) of identical RF architectures. The arrays differ only in the implementation of the biasing network and substrate metalization thickness.

II. Amplifier Array Design

The quasi-optical amplifier array schematic is shown in Fig. 1. An array has 36 9-mm unit cells arranged in a 6x6 triangular lattice. In each unit cell, the input slot antenna receives power from an incident vertically-polarized plane wave. The received power is coupled onto the 50-Ω CPW transmission line and is amplified by a commercial *Alpha* AA028P3-00 MMIC amplifier. The amplifier has a measured 22-dB small-signal gain and 16-dBm saturated output power at the 1-dB compression point. The amplified power is re-radiated in the horizontal polarization by the output slot antennas and is the coherent combination of all element outputs. Isolation and stability is provided by the orthogonally polarized input and output antennas.

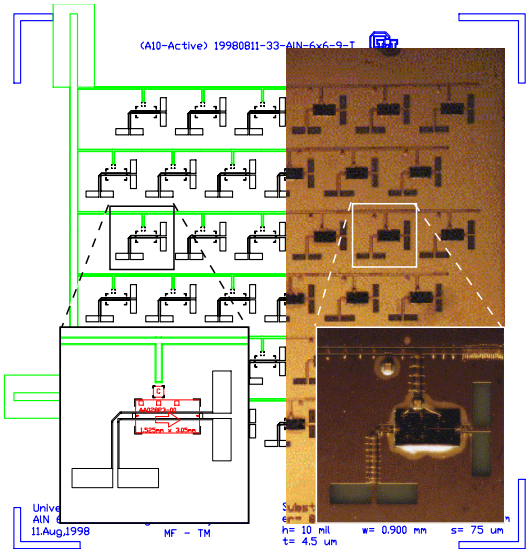

Fig. 1. Schematic of the array is shown next to a photograph of Array B with corresponding unit cell enlarged. A unit cell is 9 mm ($0.9\lambda_0$) square.

III. Fabrication

Arrays A and B were fabricated using photolithography from the same mask. The MMICs and capacitors are bonded to the substrate with silver epoxy. Each of the unit cells in both arrays have 25 gold bond wires in identical configurations. The bond wires provide connections between the MMIC pads, capacitor pads, and array metalization, as well as airbridges along the CPW lines to suppress slot modes.

This work is supported by Lockheed-Martin under a DARPA MAFET3 Program. We are grateful to John Hubert and Lee Mirth of Lockheed Martin, Orlando for their assistance throughout the project. We are grateful to Amir Mortazawi, Sean Ortiz, and Eric Schlecht for useful discussions.

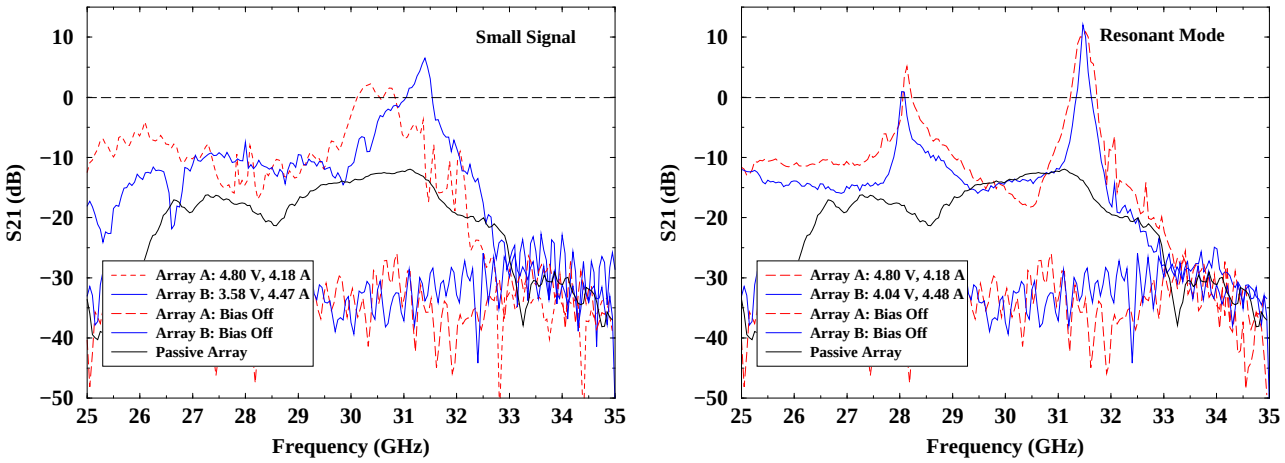

Fig. 2. Small-signal gain measurements **(a)** and resonant-mode gain measurements **(b)**. Measurements are with respect to a through calibration.

The arrays differ in metal thickness and bias line configuration. The substrate used for Array A has 4 μm of gold. To compensate for voltage variations measured along the bias network due to ohmic losses, a supplementary bias line network consisting of insulating adhesive mylar and copper tape is added. The substrate for Array B has 4.3 μm of copper with an additional 2-μm layer of electroplated gold. The thicker metal reduces the DC-bias-network voltage variation. Array B has additional airbridges and a capacitor along the bias line to enhance stability by reducing RF coupling to the bias line.

IV. Experimental Results

In this section, experimental results on the two arrays are presented. In specific, the following is discussed: small-signal gain, resonant-mode gain, saturated output power, and far-field patterns.

The small-signal gain measurement was performed using two 21.5-dB cross-polarized standard horn antennas placed $60\lambda_0$ from either side of the array. All gain measurements are relative to a free-space through. Fig. 2(a) shows the measured gain of the passive and active arrays with respect to a through calibration. Measurements are summarized in Table I(a). Similar gains were measured for near-field hard-horn excitation [7].

The term "resonant mode" is used here to describe a second stable high-gain mode of the amplifier. This mode is characterized by a narrow-band peak in gain. This mode occurs repeatably when the arrays are tuned with polarizers to 31.5 GHz. The mode is further enhanced by rotating the arrays 15° off center in the E-plane. The measured gain of the amplifiers operating in resonant-mode under small-signal excitation is shown in Fig. 2(b), and summarized in Table I(b). The cause of this mode is currently under investigation and will be expanded upon in the following paper and discussed at the conference.

TABLE I

Small-signal gain **(a)**, resonant-mode gain **(b)**, and saturated power **(c)** measurements. BW indicates the range over which the arrays have gain. G_a is the gain with respect to a passive array.

(a) Small-signal gain measurements.

Array	freq (GHz)	Gain (dB)	BW (GHz)	On/Off Ratio (dB)	G_a (dB)
A	30.40	2.2	0.71	34	10
B	31.40	6.5	0.50	38	14

(b) Resonant-mode gain measurements.

Array	freq (GHz)	Gain (dB)	BW (GHz)	On/Off Ratio (dB)	G_a (dB)
A	31.52	10.7	0.48	44	25
B	31.47	11.8	0.26	40	25

(c) Saturated power measurements.

Array	freq (GHz)	EIRP (dBm)	EIRP (W)	P_t (dBm)	P_t (mW)
A	30.40	51.0	127	26.5	451
B	31.15	51.4	139	26.9	494

Far-field large-signal power measurements are performed using a synthesized sweeper driving a *Litton* M-762-00 MMPM to saturate the array while operating in standard small-signal mode. The EIRP and output powers are summarized in Table I(c). Calculation of the transmitted array power, P_t, assumes an array gain of 24.5 dB. This value is obtained by applying the Krauss aproximation to the large-signal far-field patterns shown in Fig. 3 and subtracting 1.5 dB for the measured polarizer loss. This value agrees closely with the gain calculated from the array's physical area [8].

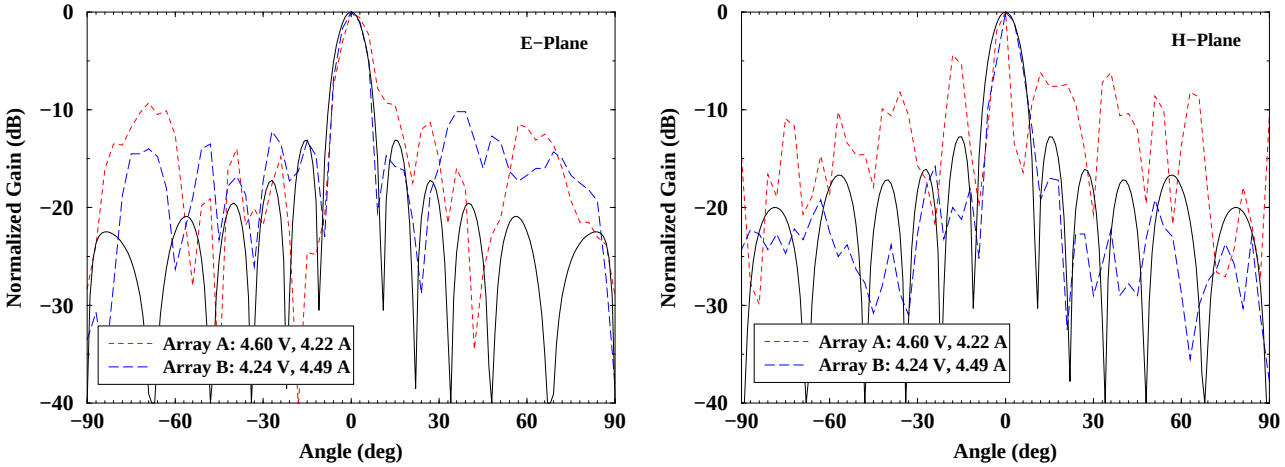

Fig. 3. E-plane far-field radiation pattern **(a)** and H-plane far-field radiation pattern **(b)**. The measurement frequency is 31.4 GHz.

Pattern measurements are performed using far-field standard-horn antennas $60\lambda_0$ from the array. Measurements are performed with polarizers under large-signal excitation. The theoretical and measured E- and H-plane patterns for the active arrays are shown in Fig. 3. Theoretical array patterns are generated by multiplying the array factor by the pattern of the slot antenna.

Although one would expect large sidelobes with a $0.9\lambda_0$ unit cell, side lobes in both planes are minimized. The array's triangular lattice minimizes the side lobes in the E-plane. In the H-plane, side lobes are eliminated due to the torroidal radiation pattern of the slot antenna. It is believed that the difference between theoretical and active patterns is due to a variation of magnitude and phase at the output of the MMICs.

V. Conclusions

This work demonstrates the ability to combine low-power commercial MMICs to achieve watt-level powers. In saturation, the arrays both deliver 140 W EIRP or 0.5 W of output power at 30.40 GHz and 31.15 GHz. In resonant mode, the amplfiers have small-signal gains of 10.7 dB at 31.52 GHz and 11.8 dB at 31.47 GHz. A variation of bias across the arrays due to the differing DC-bias networks leads to a variation in magnitude and phase at the MMIC outputs. It is believed that these variations contribute to the different peak gains, powers, and far-field patterns. To enhance stability and increase power, in future work, MMICs with lower gain and higher power will be used.

References

[1] Robert A. York, "Quasi-optical power combining," in *Active and Quasi-optical arrays for solid-state power combining*, Robert A. York and Zoya B. Popović, Eds., chapter 1. John Wiley, New York, 1997.

[2] Zoya Popović and Amir Mortazawi, "Quasi-optical transmit/receive front ends," *IEEE Trans. Microwave Theory Tech.*, vol. 46, no. 11, pp. 1964–1975, Nov. 1998.

[3] J. Hubert, J. Schoenberg, and Z. Popović, "High-power hybrid quasi-optical Ka-band amplifier design," *IEEE MTT-S Int. Microwave Symp. Dig.*, pp. 585–588, May 1995.

[4] C. M. Liu, E. A. Sovero, W. J. Ho, J. A. Higgins, M. P. De Lisio, and D. B. Rutledge, "Monolithic 40-GHz 670-mW HBT grid amplifier," *IEEE MTT-S Int. Microwave Symp. Dig.*, pp. 1123–1126, June 1996.

[5] M. P. De Lisio, S. W. Duncan, D. W. Tu, S. Weinreb, C. M. Liu, and D. B. Rutledge, "A 44-60 GHz monolithic pHEMT grid amplifier," *IEEE MTT-S Int. Microwave Symp. Dig.*, pp. 1127–1130, June 1996.

[6] E. A. Sovero, J. B. Hacker, J. A. Higgins, D. S. Deakin, and A. L. Sailer, "A Ka-band monolithic quasi-optic amplifier," *IEEE MTT-S Int. Microwave Symp. Dig.*, pp. 1453–1456, June 1998.

[7] M. A. Forman, T. S. Marshall, and Z. Popović, "Two Ka-band quasi-optical amplifier arrays," *IEEE MTT-S Int. Microwave Symp. Dig.*, June 1999.

[8] Mark A. Gouker, "Spatial power combining," in *Active and Quasi-optical arrays for solid-state power combining*, Robert A. York and Zoya B. Popovic, Eds., chapter 2. John Wiley, New York, 1997.